SIMULATION OF UPWELLING THERMAL RADIATION SCATTERED BY AEROSOL ALLOWING FOR SURFACE TEMPERATURE INHOMOGENEITIES. II. LARGE-SCALE GRADIENTS

S.V. Afonin, V.V. Belov, and I.Yu. Makushkina

Institute of Atmospheric Optics,
Siberian Branch of the Russian Academy of Sciences, Tomsk
Received July 3, 1995

Results of simulation of thermal radiation scattered by the aerosol in the 3.7 and 10.8 μm spectral channels have been analyzed taking into account large-scale gradients of surface temperature under various optical-geometric conditions of observation. The situations have been identified in which the contribution from the gradients to the radiative temperature exceeds 0.5°. A conclusion has been drawn that the temperature inhomogeneites may be ignored when remote measurements in the 10.8 μm channel are corrected for the atmospheric contribution. The effect of the atmosphere on the quality of the ocean surface temperature data obtained from the NOAA satellites has been estimated.

1. INTRODUCTION

Under natural conditions, the spatial structure of the IR radiation field of an underlying surface may be rather complicated in character due to a wide range of variations of spatial scale and magnitude of the surface temperature inhomogeneities. In this connection, it is appropriate to classify some characteristic types of the underlying surfaces for which the study of the problem being considered in this paper may yield significant practical result. Among these are the commonly encountered large-scale temperature gradients at the interface between two extended quasihomogeneous regions of the underlying surface (for example, at the "land–sea" or "surface–dense fog" interface). In this case in remote sensing of the surface through a turbid atmosphere the radiation of warmer or colder regions (relative to an observation point) will introduce the distortions caused by aerosol scattering into a signal recorded by a device and will affect the quality of the correction of remote measurements for the effect of the atmosphere. Calculations carried out in this paper allow us to estimate such an adverse effect.

2. BASIC CHARACTERISTICS OF SIMULATION

By the method of statistical simulation, the intensity J_λ and radiative temperature T_λ of natural radiation of the system "atmosphere − underlying surface" were calculated

$$J_\lambda = J_\lambda^0 + J_\lambda^{MS}, \qquad T_\lambda = B_\lambda^{-1} [J_\lambda], \qquad (1)$$

$$J_\lambda^0 = J_{ATM}^0 + J_{SURF}^0, \qquad J_\lambda^{MS} = J_{ATM}^{MS} + J_{SURF}^{MS}, \qquad (2)$$

$$J_{SURF}^0 = B_\lambda [T_S(x_0, y_0)] \exp(-\tau), \qquad (3)$$

$$J_{SURF}^{MS} = \iint\limits_S h_\lambda(x, y) \, B_\lambda [T_S(x, y)] \, dx \, dy. \qquad (4)$$

Here J_{ATM}^0, J_{SURF}^0, J_{ATM}^{MS}, and J_{SURF}^{MS} are the contributions from the atmosphere and the underlying surface to the intensity of nonscattered (J_λ^0) and scattered (J_λ^{MS}) radiation, x_0 and y_0 are the coordinates of the observation point, τ is the optical thickness of the atmosphere, B_λ is the Planck function, B_λ^{-1} is the inverse Planck function, T_S is the temperature of the underlying surface, $h(x, y)$ is the point spread function, and S is the effective spatial region of existence of the adjacency effect. In our calculations, S was bounded by a circle of radius R with the center at the observation point. The value of R was equal to 10 km for the near-ground aerosol and 100 km for the stratospheric (volcanic) aerosol,[1] which corresponds to an error of the order of 0.05° in simulation of the radiative temperature.

A model of the inhomogeneous underlying surface was specified in the following manner. The domain of existence of the adjacency effect was subdivided into two homogeneous subdomains with temperatures T_S (with an area of S_1) and $T' = T_S + dT_S$ (with an area of S_2), where $S_1 > S_2$, and the observation point was in domain S_1. This model is characterized by two geometric parameters:

a) the distance r between the dividing line and the point (x_0, y_0),

b) the azimuth angle φ' between the projection of the receiver's optical axis (ROA) on the underlying surface and the dividing line.

The increase of the distance r leads to the increase of the area S_1 and the decrease of the area S_2. The angle φ ($\varphi = 90° - \varphi'$) is the azimuth angle of the point spread function,[1] and $\varphi = 0°$ corresponds to the situation when the ROA projection is perpendicular to the dividing line but does not intersect it. Then the intensity of the adjacency effect defined by Eq. (4) for the inhomogeneous surface can be represented in the form

$$J_{\text{SURF}}^{\text{MS}} = \iint\limits_{S_1} (...) \, \mathrm{d}x \, \mathrm{d}y + \iint\limits_{S_2} (...) \, \mathrm{d}x \, \mathrm{d}y.$$

Results of simulation of the point spread function $h(x, y)$, used for calculations of $J_{\text{SURF}}^{\text{MS}}$ and description of its properties, were presented in the first part of this paper.[1] The algorithm for direct simulation on conjugate trajectories[2] was used for calculations of $J_{\text{ATM}}^{\text{MS}}$.

For convenient practical interpretation, results of analysis are presented as dependence of the temperature corrections

$$\delta T_\lambda = T_\lambda \big|_{\mathrm{d}T_S = 0} - T_\lambda \big|_{\mathrm{d}T_S \neq 0}$$

on the parameters of the temperature inhomogeneities r and T_S under various optical-geometric conditions of observation.

3. OPTICAL-GEOMETRIC CONDITIONS OF SIMULATION

Simulation was carried out under the following optical-geometric conditions of observation: spectral channels $\lambda = 3.75$ and $10.8 \, \mu m$, zenith angles of observation $\theta = 0, 30, 40$, and $55°$, the range of variation of distances $r = 0 - 10$ km for the near-ground aerosol and $r = 0 - 100$ km for the stratospheric (volcanic) aerosol, azimuth angles of observation $\varphi = 0$, 60, 120, and $180°$, and an altitude of observation of 800 km. The atmosphere was assumed cloudless, molecular–aerosol, spherically symmetric, vertically stratified, and horizontally homogeneous; meteorological model of the atmosphere was used for the mid-latitude in summer. Aerosol models were used for the marine aerosol in the 0—2 km ground atmospheric layer (for the meteorological visibility range $S_M = 2$-50 km) and the background or postvolcanic stratospheric aerosol with moderate, high, and extreme content.

The underlying surface was taken as Lambertian surface composed of two homogeneous regions emitting as black bodies with temperatures T_S and $T_S + \mathrm{d}T_S$. The magnitude of the temperature gradient varied from -20 to $+20$ K.

The data used in calculations of optical-meteorological models of the atmosphere are illustrated in detail by Fig. 1 of Ref. 1.

4. SIMULATION RESULTS

Let us consider the temperature corrections calculated as functions of the distance r between the point of observation and the dividing line, temperature gradient $\mathrm{d}T_S$, azimuth angle φ, zenith angle θ, and optical thickness of aerosol scattering τ_{sct}. First of all, we notice that the temperature gradients may markedly affect the radiative temperature T_λ. So, at the angles $\theta = 0$–$55°$ the maximum values of δT_λ (at the interface), according to our estimates, are equal to ~ 4.1–$5.4°$ ($\lambda = 3.75 \, \mu m$) and ~ 0.7–$1.2°$ ($\lambda = 10.8 \, \mu m$) for the near-ground aerosol and ~ 1.3–$3.6°$ ($\lambda = 3.75 \, \mu m$) and ~ 0.2–$0.7°$ ($\lambda = 10.8 \, \mu m$) for the stratospheric aerosol.

Results of calculations of the radiative temperature contrast T_λ at the interface are tabulated in Table I for $\mathrm{d}T_S = +20°$. In the upper row of the table the difference between T_λ for homogeneous surfaces with temperatures T_S and $T_S + \mathrm{d}T_S$ is given. Comparing the data of the upper and lower rows, a conclusion should be drawn that an account of mutual contribution of radiation scattered by an adjacent region of the surface may result in essential decrease of the temperature contrast.

Analysis of the data shown in Fig. 1 allows us to identify some characteristic features in the behavior of δT_λ depending on the distance r and azimuth angle φ. For more vivid presentation, the results of $\delta T_\lambda(r)$ calculation are illustrated separately by plots inserted in Fig. 1 for the near-ground aerosol with $r \leq 1$ km.

The temperature correction δT_S is a monotonically decreasing function of the distance r for both types of aerosols, with the rate of $\delta T_\lambda(r)$ decrease being determined by the parameters θ, φ, and τ_{sct}. In particular, the rate of decrease of δT_λ is slowed down with increasing θ. The azimuth dependence of the temperature correction is characterized by the maximum values of δT_λ at $\varphi = 180°$ for $r < r_1$ and at $\varphi = 0°$ for $r > r_2$. The minimum of the function $\delta T_\lambda(\varphi)$ occurs at distances $r < r^*$ and $\varphi = 0°$, but its position shifts gradually with a further increase in r. The values of r_1, r_2, and r^* are determined by the optical-geometric parameters of observation. An exception is the case of the stratospheric aerosol for $\lambda = 10.8 \, \mu m$ at $\theta > 30°$, when the function $\delta T_\lambda(\varphi)$ reaches its maximum at $\varphi = 180°$ practically for the entire range of distances r and its minimum at $\varphi = 0°$.

It also should be noted that the difference between $\delta T_\lambda(\varphi = 0°)$ and $\delta T_\lambda(\varphi = 180°)$ exceeds the significance level ($\sim 0.5°$) at distances ~ 1 km at $\theta = 45°$ ($\mathrm{d}T_S > 15°$, $S_M \sim 2$-3 km) and ~ 1–3 km at $\theta = 55°$ ($\mathrm{d}T_S > 5°$, $S_M \sim 2$–10 km) in the case of the near-ground aerosol. In the case of the volcanic aerosol, azimuth differences exceeds $0.5°$ at distances 10–15 km at $\theta = 45°$ ($\mathrm{d}T_S > 15°$) and 15–40 km at $\theta = 55°$ ($\mathrm{d}T_S > 10°$).
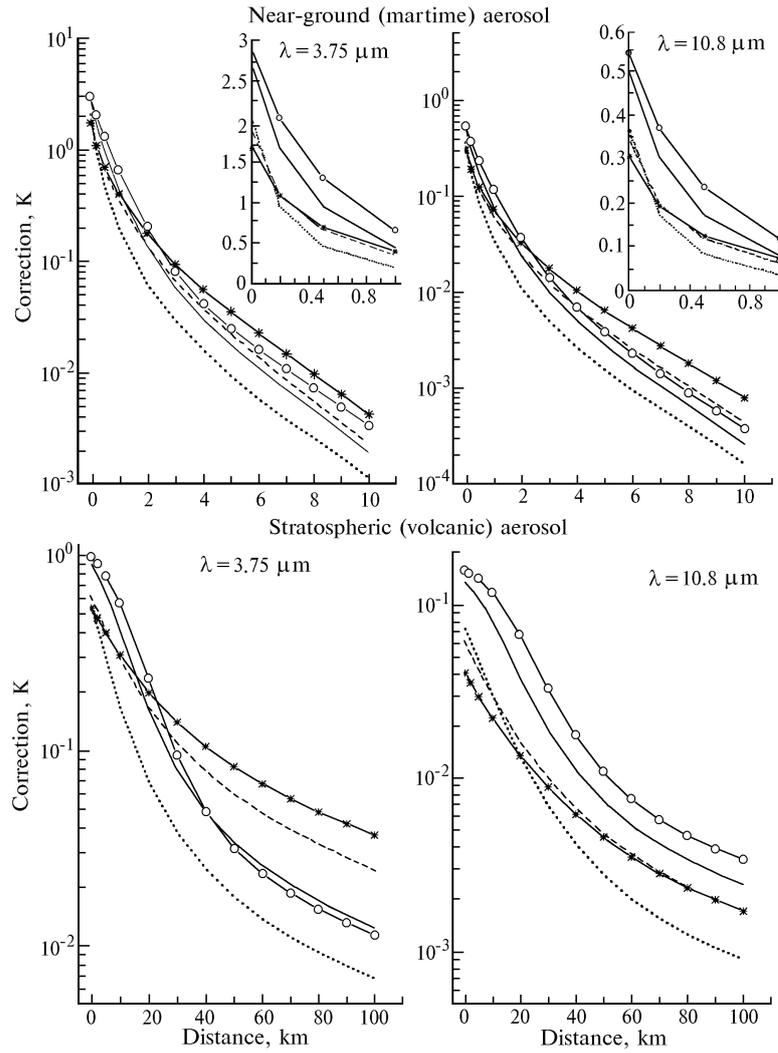
FIG. 1. Dependence of $\delta T_\lambda(r)$ for near-ground ($S_M = 5$ km) and stratospheric (high-concentration) aerosols for the temperature gradient $dT_S = +20°$ at zenith angles $\theta = 0°$ (dotted curves) and 45° and azimuth angles $\varphi = 0$ (asterisks), 60 (dashed curve), 120 (solid curve), and 180° (empty circles).

TABLE I.

	Aerosol					
	Near-ground			Stratospheric		
$\theta,°$	$S_M = 2$ km	$S_M = 5$ km	$S_M = 10$ km	Extreme	High	Moderate
	$\lambda = 3.75$ μm					
0	14.16	15.36	15.99	17.09	17.15	17.18
	7.19	11.99	14.25	14.93	16.31	16.88
45	11	13	14.10	16.02	16.13	16.18
	4.18	9.27	12.10	13.31	15.04	15.85
55	7.98	10.24	11.79	14.89	14.97	15.01
	1.80	6.38	9.64	11.45	13.58	14.59
	$\lambda = 10.8$ μm					
0	13.17	14.05	14.36	14.20	14.53	14.67
	11.72	13.35	13.96	13.81	14.39	14.62
45	10.04	11.28	11.74	11.61	12.04	12.23
	8.46	10.48	11.28	11.11	11.86	12.17
55	6.85	8.27	8.83	8.84	9.28	9.47
	5.31	7.43	8.34	8.16	9.02	9.39

Near-ground (maritime) aerosol

Stratospheric (volcanic) aerosol

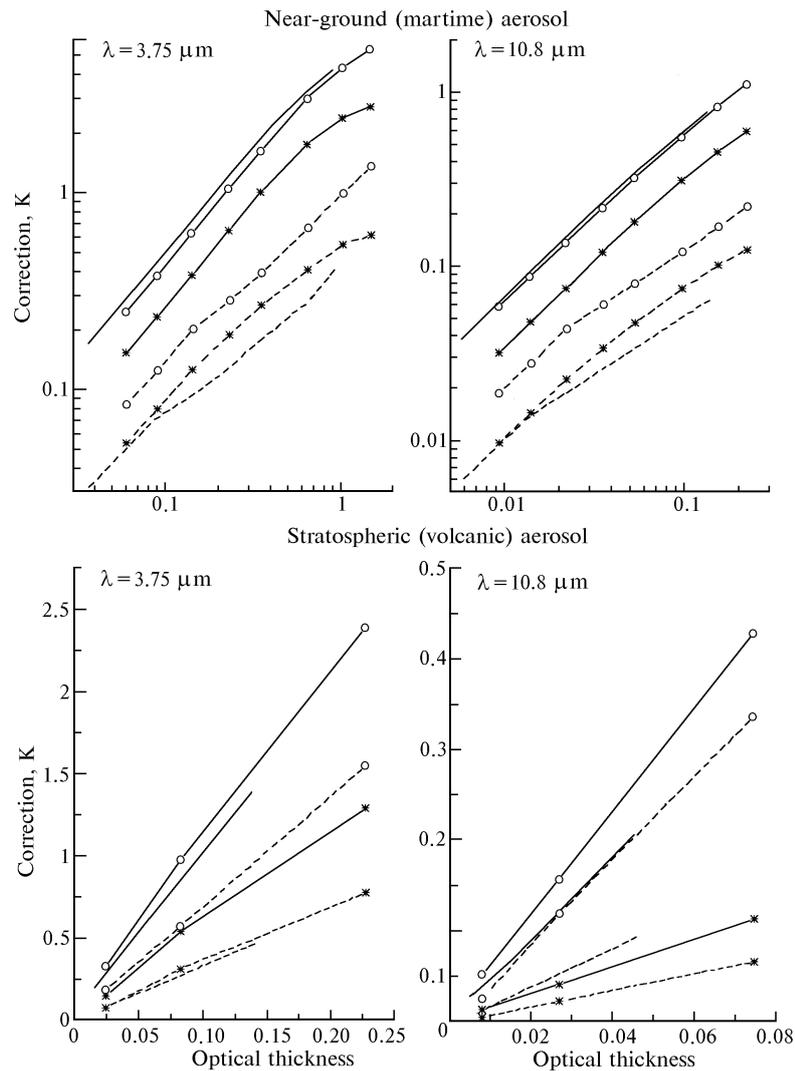*FIG. 2. Dependence of $\delta T_\lambda(\tau_{sct})$ in the case of near-ground ($S_M = 5$ km) and stratospheric (high-concentration) aerosols for the temperature gradient $dT_S = +20°$ at zenith angles $\theta = 0°$ and $45°$ (indicated by symbols), azimuth angles $\varphi = 0$ (asterisks) and $180°$ (empty circles), and distances $r = 0$ (dashed curve), 1 (solid curve, the near-ground aerosol), and 10 km (solid curve, the stratospheric aerosol).*

The maximum difference between $\delta T_\lambda(\varphi = 0°)$ and $\delta T_\lambda(\varphi = 180°)$ may reach 2.5–2.8° in the channel $\lambda = 3.76$ μm, whereas it is no more than 0.6–0.9° in the channel $\lambda = 10.8$ μm.

Now we analyze the influence of optical thickness of aerosol scattering on the corrections δT_λ for various r with the use of data shown in Fig. 2. It follows from these data that δT_λ increases monotonically with increasing τ_{sct} for the entire range of distances $0 \leq r \leq r^*$ (where $r^* \sim 1$ and 10 km for the near-ground and volcanic aerosol, respectively), which determines the domain of significant (from a practical point of view) influence of the temperature gradients on T_λ. However, a tendency to violate the monotony of $\delta T_\lambda(\tau_{sct})$, like in the case of point spread function,[1] becomes pronounced for low visibility ranges and

near-ground aerosols. The shape of the curves $\delta T_\lambda(\tau_{sct})$ allows us to assume that the dependence $\delta T_\lambda(\tau_{sct})$ may be described by a power-law function, whereas a linear approximation is reasonable for the volcanic aerosol.

Describing the relations of temperature corrections δT_λ with the optical-geometric parameters r, θ, φ, and τ_{sct}, their good agreement with analogous dependence of the point spread function on these parameters[1] should be emphasized.

We will consider the influence of the temperature gradient dT_S on the magnitude of δT_λ (see Fig. 3). In the figure, the curves calculated at $\theta = 0°$ and $r = 10$ km ($\lambda = 3.75$ μm) for the volcanic aerosol merge with the curves calculated at $\varphi = 0°$ and $r = 10$ km and $\varphi = 180°$ and $r = 0$ km. Analysis of the curves

shown in Fig. 3 demonstrates that the function $\delta T_\lambda(dT_S)$ is nonlinear in the channel $\lambda = 3.75$ μm and practically linear in the channel $\lambda = 10.8$ μm, which is determined by the temperature dependence of Planck's function in these spectral regions. In this connection, the absolute values of the temperature

corrections in the channel $\lambda = 3.75$ μm may differ noticeably for gradients being equal in magnitudes but opposite in signs. So, the maximum difference reaches 1.9–2.4° for the near-ground aerosol and 0.7–1.7° for the stratospheric aerosol at $\varphi = 180°$ and $\theta = 0$–55°.
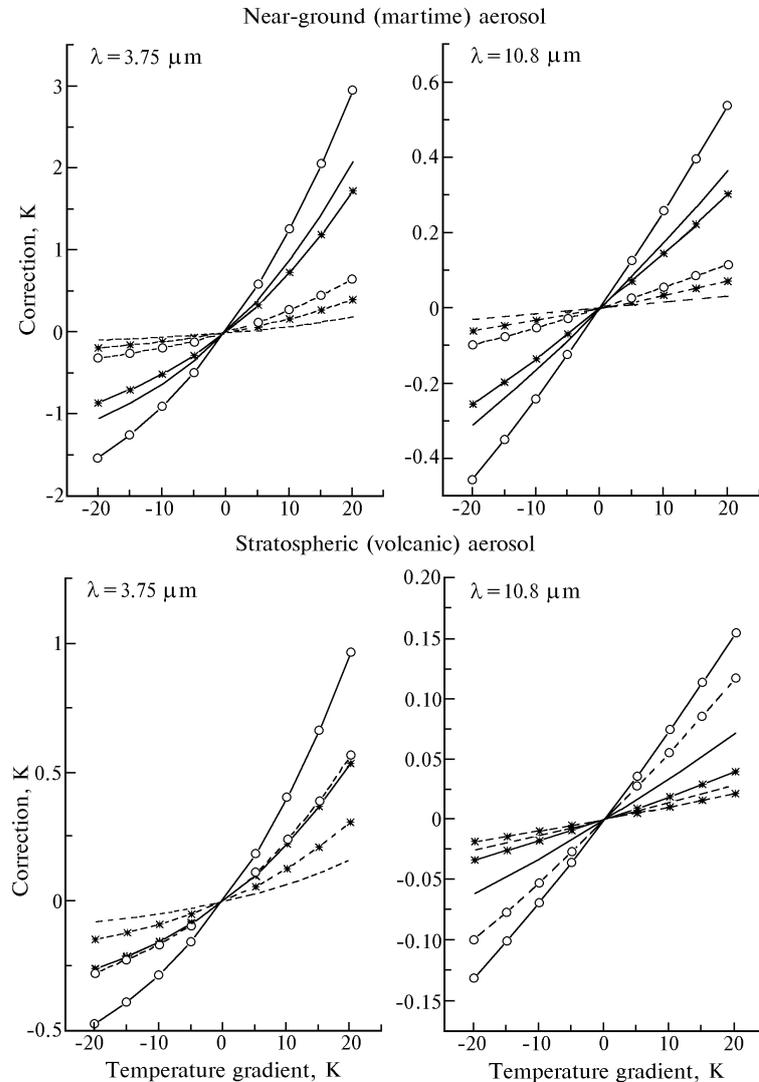

FIG. 3. Dependence of δT_λ on dT_S for near-ground ($S_M = 5$ km) and stratospheric (high-concentration) aerosols at zenith angles $\theta = 0°$ and $45°$ (indicated by symbols), azimuth angles $\varphi = 0$ (asterisks) and $180°$ (empty circles), and distances $r = 0$ (dashed curve), 1 (solid curve, the near-ground aerosol), and 10 km (solid curve, the stratospheric aerosol).

Generalizing the preceding, a conclusion can be drawn that the temperature gradients influence the quality of correction of remote measurements in the channel 10,8 μm for the effect of the atmosphere only under "extreme" conditions of observation ($S_M < 5$ km, $\theta > 45°$, $dT_S \approx 20°$ and $r \leq 0.5 - 1$ km). Consequently, to correct the data of satellite remote sensing of the underlying surface (recorded with spatial resolution of 0.5–1.0 km), the adverse effect caused by temperature inhomogeneities should be considered

primarily in the channel $\lambda = 3.75$ μm. In so doing, the relative positions of the point of observation and the interface should be taken into consideration, as well as the orientation of the receiver's optical axis and magnitude and sign of the temperature gradient.

Estimates of r_{max} such that the condition $\delta T_\lambda(r) > 0.5°$ is satisfied at $r > r_{max}$, may be of interest for users of the data of IR remote sensing of the underlying surface. These data are shown for the
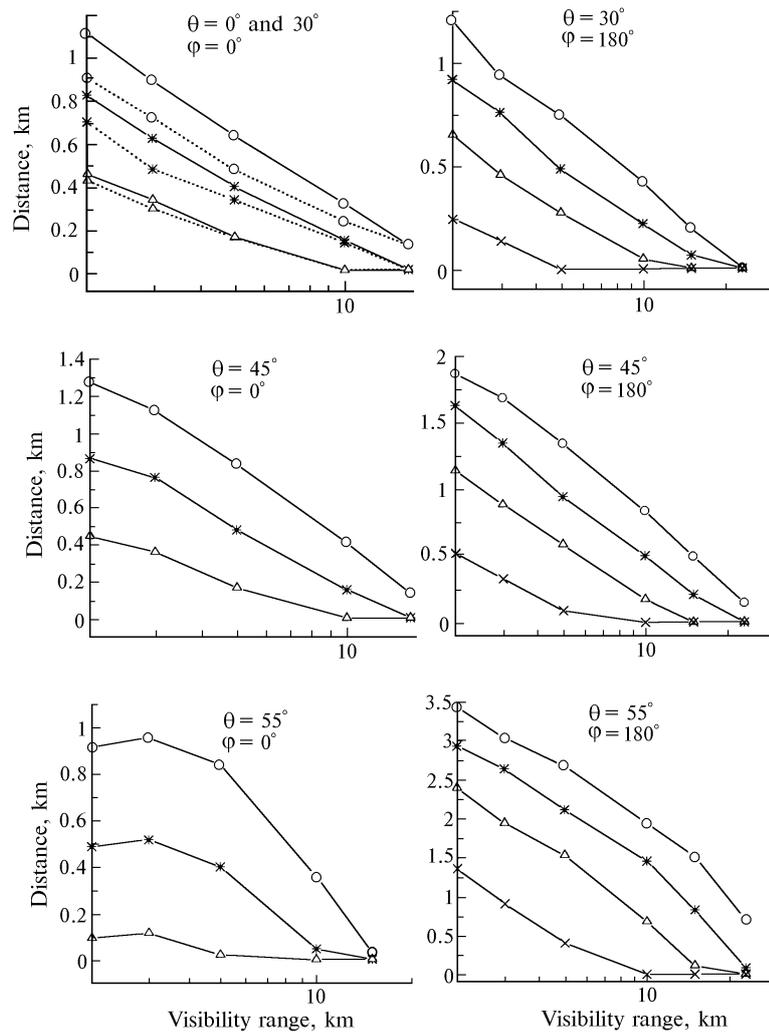
FIG. 4. *Dependence of* r_{max} *on the optical thickness* τ_{sct} *for the near-ground aerosol* ($\lambda = 3.75$ μm) *at zenith angles* $\theta = 0$ *(dashed curve), 30, 45, and 55° and azimuth angles* $\varphi = 0$ *and 180° for the temperature gradient* $dT_S = +20$ *(empty circles), +15 (asterisks), +10 (triangles), and +5° (crosses).*

TABLE II.

Gradient dT_S						
Aerosol	$\varphi = 0°$			$\varphi = 180°$		
content	+ 20°	+ 15°	+ 10°	+ 20°	+ 15°	+ 10°
$\theta = 0°$						
Extreme	9.406	6.048	1.490	—	—	—
High	0.807	0	0	—	—	—
$\theta = 30°$						
Extreme	14.554	8.119	1.472	15.028	10.245	5.316
High	1.209	0	0	4.433	0	0
$\theta = 45°$						
Extreme	20.666	11.648	1.391	25.374	19.901	14.254
High	1.293	0	0	12.089	6.277	0
$\theta = 55°$						
Extreme	27.986	14.019	0	49.908	44.411	36.163
High	0	0	0	31.274	24.727	11.663

channel $\lambda = 3.75$ μm   in   Fig. 4   (the   near-ground aerosol) and in Table II (the stratospheric aerosol).

Analysis   of   the   values   of r_{max} allows   us,   for example,   to   estimate   the   distorting   effect   of   the

temperature gradients on the quality of data on the oceanic surface temperature (OST) measured at regular intervals from the NOAA satellites in channels $\lambda = 3.75$, 10.8, and 12.0 μm with the use of the AVHRR device with spatial resolution of the order of 1 km for local data (LAC data) and of the order of 4 km for global data (GAC data). The procedure for automatic processing of OST global measurements[3] includes, in addition to algorithms for atmospheric correction, some tests for data rejection.

The so-called land / sea test, which obviates the need for the correction for the atmosphere when pixels are spaced at distances shorter than 10 km (day, $\lambda = 10.8$ and 12.0 μm) or 50 km (night, $\lambda = 3.75$, 10.8, and 12.0 μm) from the land–sea interface is among them. Analysis of values of r_{max} allows us to draw a conclusion that this test must eliminate the distorting effect of natural land radiation scattered by the aerosol

on the quality of global data on OST for the entire range of variations of the considered optical-geometric conditions. However, mapping of OST of the coastal region on the basis of high-resolution local remote data calls for consideration of this distorting factor to correct the data for the effect of the atmosphere.

REFERENCES

1. S.V. Afonin, V.V. Belov, and I.Yu. Makushkina, Atmos. Ocenaic Opt. **8**, No. 9, 756–762 (1995).
2. V.V. Belov and I.Yu. Makushkina, in: *Theory and Applications of Statistical Simulation* (Publishing House of the Computing Center of the Siberian Branch of the Russian Academy of Sciences, Novosibirsk, 1988), pp. 153-164.
3. P.E. McClain,   W.G. Pichel,   and   C.C. Walton, J.Geophys. Res. **90**, No. C6, 11587–11601 (1985).